



Universität St.Gallen

A variance spillover analysis without  
covariances: what do we miss?

Matthias R. Fengler, Katja I. M. Gisler

April 2014 Discussion Paper no. 2014-09

Editor: Martina Flockerzi  
University of St.Gallen  
School of Economics and Political Science  
Department of Economics  
Bodanstrasse 8  
CH-9000 St. Gallen  
Phone +41 71 224 23 25  
Fax +41 71 224 31 35  
Email [seps@unisg.ch](mailto:seps@unisg.ch)

Publisher: School of Economics and Political Science  
Department of Economics  
University of St.Gallen  
Bodanstrasse 8  
CH-9000 St. Gallen  
Phone +41 71 224 23 25  
Fax +41 71 224 31 35

Electronic Publication: <http://www.seps.unisg.ch>

A variance spillover analysis without covariances:  
what do we miss?

Matthias R. Fengler, Katja I. M. Gisler

Author's address:

Prof. Dr. Matthias R. Fengler  
Institute of Mathematics and Statistics  
Bodanstrasse 6  
CH-9000 St. Gallen  
Phone +41 71 224 24 57  
Fax +41 71 224 28 94  
Email [matthias.fengler@unisg.ch](mailto:matthias.fengler@unisg.ch)  
Website [www.mathstat.unisg.ch](http://www.mathstat.unisg.ch)

Katja I. M. Gisler  
Institute of Mathematics and Statistics  
Bodanstrasse 6  
CH-9000 St. Gallen  
Phone +41 71 224 24 94  
Email [katja.gisler@unisg.ch](mailto:katja.gisler@unisg.ch)  
Website [www.mathstat.unisg.ch](http://www.mathstat.unisg.ch)

## **Abstract**

We evaluate the relevance of covariances in the transmission mechanism of variance spillovers across the US stock, US bond and gold markets from July 2003 to December 2012. For that purpose, we perform a comparative spillover analysis between a model that considers covariances and a model that considers only variances. Our results emphasise the importance of covariances. Including covariances leads to an overall increase of the spillover level and detects the beginnings of the financial crisis and of the US debt ceiling crisis earlier than the spillover measure that considers only variances. Even for the low-dimensional system that we consider, one misses important variance spillover channels when covariances are excluded.

## **Keywords**

Covariance spillovers, financial crisis, sovereign debt crisis, spillover index, variance decomposition, vector autoregression, variance spillovers.

## **JEL Classification**

C01, C32, G01, G15.

# 1. Introduction

The recent financial and sovereign debt crises have made the interdependence of global markets apparent once again. Starting in the US, the subprime mortgage worries that peaked with the collapse of Lehman Brothers in September 2008 have been propagated through the markets and have resulted in a global financial crisis, whose most recent ramifications are the US and European sovereign debt crises. Such crises usually come along with a regular pattern. Their most notable signal is the significant increase in volatility reflecting the increased uncertainty and activity in the markets. Moreover, volatility usually spreads from one market to others. Therefore, the measuring and monitoring of volatility or variance and its spillovers is of particular interest not only to regulators and policy makers, but also to asset and risk managers.

The most widespread techniques used to model spillovers are correlation or covariance models such as the (dynamic) conditional correlation model of [Engle \(2002\)](#) or the BEKK model of [Engle and Kroner \(1995\)](#). However, these concepts measure pairwise and linear relationships and are thus of limited use in a setting involving several variables that exhibit potentially nonlinear characteristics as is typical for financial data. Alternative specifications circumventing this difficulty include, for example, the dynamic equi-correlation approach of [Engle and Kelly \(2012\)](#) which uses the average across correlations and thus avoids taking pairwise associations. Similarly, the literature on systemic risk has recently introduced spillover measures, such as the systemic expected shortfall proposed by [Acharya, Pedersen, Philippon and Richardson \(2010\)](#), the distressed insurance premium presented by [Huang, Zhou and Zhu \(2011\)](#), or the conditional value at risk of [Adrian and Brunnermeier \(2011\)](#). Although these measures allow for nonlinear dependence, they only quantify associations between individual and system-wide dependencies. More recently, [Diebold and Yilmaz \(2012, 2014\)](#) developed a unified framework for measuring spillovers that allows one not only to track previous and current crises, but, more importantly, to measure spillovers at levels other than the pairwise level, through system-wide spillovers, in a coherent way.

The analytical tools of the Diebold-Yilmaz framework are system-wide spillovers and (pairwise) directional spillover measures that are obtained from the forecast-error variance decomposition of an underlying vector autoregressive model (VAR). Studies using this method to analyse volatility or variance spillovers are therefore

based on vector autoregressive models of volatilities or variances; see, e.g., Diebold and Yilmaz (2009, 2012, 2014), Kumar (2013) and Louzis (2013). These vector autoregressive models are merely stacked univariate regression models of volatilities. The large literature on multivariate GARCH and stochastic volatility models, however, emphasises the importance of covariance dynamics. Thus, one may ask whether one misses relevant spillover information by only considering volatility or variance spillovers. We therefore propose to incorporate covariances into the model setting. In contrast to previous volatility or variance spillover studies, we exploit high-frequency data for this purpose. This allows us to estimate accurately the daily covariance matrices, which we model dynamically. We then perform a comparative spillover analysis in order to determine the relevance of covariance spillovers.

For our modelling approach, we extend the heterogeneous autoregressive (HAR) model of Corsi (2009) to the multivariate case by developing a vector HAR that is analogous to the standard vector autoregressive (VAR) model. This multivariate HAR model, which is termed the MHAR-RCov model, allows us to apply the method of Diebold and Yilmaz (2012, 2014). Moreover, in the same way as the univariate HAR model, it is able to reproduce patterns of long-range dependence in volatility while remaining parsimonious and easy to estimate; see Corsi, Audrino and Renò (2012) for a detailed discussion of this model.

Based on our models, we investigate the role of covariances in the spillover transmission mechanism between three major markets. Using a period of almost ten years for our study, we compare the variance and covariance spillovers across the US equity, the US bond and the gold markets based on the MHAR-RCov model with the variance spillovers based on a model that considers only variances. Our results highlight the importance of covariances. We find that including covariances leads to an overall increase in the spillover level. Moreover, the approach that considers covariances detects the beginnings of the financial and the US debt ceiling crises earlier than the approach that considers only variances. We can show that this earlier detection is attributable to substantial spillovers across variances and covariances that could be linked to a flight-to-quality phenomenon.

We proceed as follows. Section 2 introduces the model. Section 3 presents the methodological approach. The results of the spillover analysis are discussed in section 4. Section 5 concludes.

## 2. The model

For our analysis, we propose a multivariate version of the heterogeneous autoregressive model (HAR). Formally, the model can be written as:

$$x_t = \beta + \beta^{(1)}x_{t-1} + \beta^{(5)}x_{t-1}^{(5)} + \beta^{(22)}x_{t-1}^{(22)} + \epsilon_t \quad (1)$$

where  $x_t = \text{vech}(RCov_t^{(h)})$  is the  $N(N+1)/2 \times 1$  vector representing the unique elements of the  $N$ -dimensional realised covariance matrix for a specific time horizon  $h$ ,  $\beta^{(h)}$  is the corresponding  $N(N+1)/2 \times N(N+1)/2$  coefficient matrix and  $\epsilon_t$  is an  $N(N+1)/2 \times 1$  vector of innovations. Analogously to Corsi (2009), the  $h$ -period realised covariance matrix is defined as:

$$RCov_t^{(h)} = \frac{1}{h} \sum_{j=0}^{h-1} RCov_{t-j}, \quad (2)$$

where  $RCov_{t-j}$  is the daily realised covariance matrix as defined in Eq. (20) in Appendix A for day  $t-j$ . The cascade structure (daily, weekly, monthly) in Eq. (1) is motivated by the idea that market participants with different investment horizons are active in the market. Conceptually, our model in Eq. (1) is in the spirit of the VEC( $p, q$ )-GARCH model introduced by Bollerslev, Engle and Wooldridge (1988). We call it the MHAR-RCov model.

We also consider a model that only includes variances. This model is referred to as the MHAR-RV model, and is defined as:

$$\tilde{x}_t = \tilde{\beta} + \tilde{\beta}^{(1)}\tilde{x}_{t-1} + \tilde{\beta}^{(5)}\tilde{x}_{t-1}^{(5)} + \tilde{\beta}^{(22)}\tilde{x}_{t-1}^{(22)} + \tilde{\epsilon}_t \quad (3)$$

where  $\tilde{x}_t$  is an  $N \times 1$  vector containing the realised variances of the  $N$  variables in the system for a specific time horizon  $h$ ,  $\tilde{\beta}^{(h)}$  is the corresponding  $N \times N$  coefficient matrix and  $\tilde{\epsilon}_t$  is an  $N \times 1$  vector of innovations.

As the HAR model is a restricted AR(22) model, the MHAR-RCov and MHAR-RV models are constrained VAR(22) models that can be estimated by standard estimation techniques. The VAR(22) structure can be seen by noting that the model in

Eq. (1), and analogously the model in Eq. (3), can be written as:

$$x_t = \phi + \sum_{i=1}^{22} \phi_i x_{t-i} + \epsilon_t \quad (4)$$

where  $\phi = \beta$ ,

$$\phi_i = \begin{cases} \beta^{(1)} + \frac{1}{5}\beta^{(5)} + \frac{1}{22}\beta^{(22)} & \text{for } i = 1 \\ \frac{1}{5}\beta^{(5)} + \frac{1}{22}\beta^{(22)} & \text{for } i = 2, \dots, 5 \\ \frac{1}{22}\beta^{(22)} & \text{for } i = 6, \dots, 22. \end{cases} \quad (5)$$

The number of parameters in the MHAR-RCov model in Eq. (1) is  $3(N(N+1)/2)^2 + N(N+1)/2$ . For example, even for  $N = 3$ , the model already has 114 parameters to estimate. In order to address the curse of dimensionality, we reduce the parameter space. On the one hand, this can be achieved by economic considerations; see, e.g., [Bonato, Caporin and Angelo \(2009\)](#). On the other hand, one can impose restrictions by means of a purely data-driven approach. Among the model selection procedures discussed by [Brüggemann and Lütkepohl \(2001\)](#), [Brüggemann, Krolzig and Lütkepohl \(2002\)](#) and [Lütkepohl \(2005\)](#), we choose the sequential elimination of regressors (SER) procedure combined with the information criterion of [Schwarz \(1978\)](#).<sup>1</sup>

We apply the SER procedure to both the MHAR-RCov model and the MHAR-RV model. The final restricted MHAR-RCov and MHAR-RV models can be written as

$$x_t = \psi + \sum_{i=1}^{22} \psi_i x_{t-i} + \epsilon_t \quad (6)$$

$$\tilde{x}_t = \tilde{\psi} + \sum_{i=1}^{22} \tilde{\psi}_i \tilde{x}_{t-i} + \tilde{\epsilon}_t \quad (7)$$

with  $\psi_i = R_i \circ \phi_i$  and  $\tilde{\psi}_i = \tilde{R}_i \circ \tilde{\phi}_i$ . Here,  $R_i$  and  $\tilde{R}_i$  denote the  $N(N+1)/2 \times N(N+1)/2$  and the  $N \times N$  restriction matrices of the MHAR-RCov and the MHAR-RV models, respectively, taking the value zero when a coefficient is set to zero and one otherwise, and  $\circ$  is the Hadamard product. In the following, we use the MHAR-RCov and MHAR-RV models to refer to the restricted MHAR-RCov and the restricted MHAR-RV models, respectively.

The linear nature of the MHAR-RCov model allows for a direct interpretation of the coefficients and yields unbiased forecasts. Both features are essential for the spillover analysis.

---

<sup>1</sup>More details on the SER procedure and the choice of the selection criterion can be found in [Appendix B](#).



This is for two reasons. First, the spillover analysis is built on multi-step forecasts. Second, direct interpretability is required in order for one to be able to allocate the spillovers to their source. One could be concerned about the fact that the model fails to guarantee the positive-definiteness of the covariance matrices. However, the spillover analysis relies on the variance decomposition and not on forecasts. Therefore, the lack of positive-definiteness could only emerge as an efficiency issue. Generally, there are few multivariate variance models available that guarantee the positive-definiteness of the covariance matrix by means of nonlinear transformations. Chiriac and Voev (2011) use the Cholesky decomposition and Bauer and Vorkink (2011) the matrix log transformation. However, as a result of these non-linear transformations, these covariance models lack direct interpretability of the coefficients and yield biased forecasts, so that the spillover method of Diebold and Yilmaz (2012, 2014) cannot be applied.

### 3. Spillover measures

Diebold and Yilmaz (2009, 2012, 2014) suggest that one should assess interdependencies across markets, asset classes or countries by means of spillover measures that are based on the forecast-error variance decomposition of a vector autoregressive (VAR) model. In the light of this, consider a covariance stationary  $K$ -variable VAR( $p$ ):

$$x_t = \sum_{i=1}^p \phi_i x_{t-i} + \epsilon_t, \quad (8)$$

where  $\phi_i$  is a  $K \times K$  parameter matrix and  $\epsilon_t$  is an error term with zero mean and covariance matrix  $\Sigma$ . In our setting, we use the restricted VAR(22) as outlined in Eq. (6) and Eq. (7). Its moving average representation is given by:

$$x_t = \sum_{i=0}^{\infty} A_i \epsilon_{t-i}, \quad (9)$$

where the  $K \times K$  coefficient matrices  $A_i$  are derived from  $A_i = \phi_1 A_{i-1} + \phi_2 A_{i-2} + \phi_3 A_{i-3} + \dots + \phi_p A_{i-p}$ .

There are two approaches for deriving the variance decomposition. The first approach uses the Cholesky factor orthogonalisation that generates orthogonalised innovations and results in an order-dependent variance decomposition. The second approach exploits the generalised VAR framework of Koop, Pesaran and Potter (1996) and Pesaran and Shin (1998) that allows for correlated, instead of orthogonalised, shocks. As a result, this approach produces an order-independent variance decomposition. In contrast to the Cholesky decomposition, the generalised variance decomposition allows one to analyse the directions of spillovers.

Consequently, exploiting the generalised VAR framework is more compelling.

Following Pesaran and Shin (1998), the decomposition of the error variance into the variance components attributable to the different variables under consideration, for a forecast horizon  $H$ , is given by:

$$\theta_{ij}^g(H) = \frac{\sigma_{jj}^{-1} \sum_{h=0}^{H-1} (e_i^\top A_h \Sigma e_j)^2}{\sum_{h=0}^{H-1} (e_i^\top A_h \Sigma A_h^\top e_i)}, \quad (10)$$

where  $\Sigma$  is the covariance matrix of the error variance  $\epsilon$ ,  $\sigma_{jj}$  is the variance of the error term for the  $j$ th equation and  $e_i$  is the binary selection vector whose  $i$ th entry takes the value one and whose other entries are all zero. As the shocks to each variable are not orthogonalised, as they are for the case of the Cholesky decomposition, the sum of the contributions to the forecast-error variance is not equal to one. Diebold and Yilmaz (2012) thus propose that  $\theta_{ij}^g(H)$  should be normalised such that the information in the variance decomposition matrix can directly be used for the spillover index. This yields:

$$\tilde{\theta}_{ij}^g(H) = \frac{\theta_{ij}^g(H)}{\sum_{j=1}^N \theta_{ij}^g(H)}. \quad (11)$$

This expression represents approximately<sup>2</sup> the fraction of the  $H$ -step-ahead forecast-error variance of variable  $j$  generated by a shock to variable  $i$ . It can therefore answer the question of approximately what fraction of the  $H$ -step-ahead error variance in forecasting  $x_j$  is due to shocks to  $x_i$ . By construction, we have  $\sum_{j=1}^N \tilde{\theta}_{ij}^g(H) = 1$  and  $\sum_{i,j=1}^N \tilde{\theta}_{ij}^g(H) = N$ .

### 3.1. Spillover index

Diebold and Yilmaz (2009) define *own variance shares* and *cross variance shares* of an  $H$ -step-ahead forecast-error variance. *Own variance shares* are the fractions of the  $H$ -step-ahead forecast-error variances in forecasting variable  $i$  that are attributable to shocks to variable  $i$  for  $i = 1, \dots, K$ , while *cross variance shares* or *spillovers* are the corresponding fractions attributable to shocks to variable  $j$  for  $j = 1, \dots, K$  such that  $j \neq i$ . The spillover index is defined as the sum of the cross variance shares divided by the sum of all variance shares. The resulting spillover index for the  $H$ -step-ahead forecast horizon is hence defined as:

$$S^g = \frac{\sum_{i,j=1, i \neq j}^N \tilde{\theta}_{ij}^g(H)}{\sum_{i,j=1}^N \tilde{\theta}_{ij}^g(H)} = \frac{\sum_{i,j=1, i \neq j}^N \tilde{\theta}_{ij}^g(H)}{N}. \quad (12)$$

Essentially, this spillover index is the sum of all the off-diagonal elements of a generalised

---

<sup>2</sup>The expression is not exact as it is based on the properties of the generalised variance decomposition. With Cholesky factor identification, the expression is exact.

variance decomposition relative to the number of variables considered in the specific VAR at hand. It summarises how much of the forecast-error variances can be explained by spillovers.

### 3.2. Directional spillovers

As Diebold and Yilmaz (2012, 2014) point out, using the generalised VAR framework as opposed to the Cholesky based framework allows one to determine the direction of spillovers. The directional spillovers received by variable  $i$  from all other variables  $j$  are defined as:

$$S_{i\cdot}^g(H) = \frac{\sum_{j=1, j \neq i}^N \tilde{\theta}_{ij}^g(H)}{N}, \quad (13)$$

while the directional spillovers transmitted by variable  $i$  to all other variables  $j$  are measured by:

$$S_{\cdot i}^g(H) = \frac{\sum_{j=1, i \neq j}^N \tilde{\theta}_{ji}^g(H)}{N}. \quad (14)$$

The set of directional spillovers provides a decomposition of the spillover index into spillovers coming from (or to) a specific source. It hence allows one to identify the systemically important drivers of the spillover index, which is particularly relevant for regulators and for risk and asset managers.

### 3.3. Pairwise directional spillovers

We can further decompose the directional spillovers into pairwise directional spillovers. The pairwise directional spillovers from variable  $j$  to variable  $i$  are defined as :

$$S_{ij}^g = \frac{\tilde{\theta}_{ij}^g(H)}{N}, \quad (15)$$

and from variable  $i$  to variable  $j$  are defined as:

$$S_{ji}^g = \frac{\tilde{\theta}_{ji}^g(H)}{N}. \quad (16)$$

Note that generally  $S_{ij}^g \neq S_{ji}^g$ . The decomposition into pairwise spillovers allows us to determine the spillover linkages between two variables. We can hence identify the relevant spillover interconnections of the directional spillovers and the spillover index.

## 4. Empirical application

### 4.1. Data description

The data is obtained from Tick Data<sup>3</sup>, which offers validated tick-by-tick data on a large number of global equities, indices, options and futures. For this study we consider the T-Bond 30-year futures (US) traded on the CBOT, the S&P 500 index futures (SP) listed on the CME and the COMEX gold futures (GC). The data set covers the tick-by-tick transaction prices of these futures from July 2003 to December 2012.

Before constructing the covariance matrices, some adjustments are made to the raw five-minute return series. First, only overlapping trading hours are considered. This simultaneous filter criterion needs to take into account not only the different trading hours of the three futures under consideration, but also two different time zones, due to the locations of the exchanges where the futures are traded. This results in an observation time window of 14:35 GMT to 18:30 GMT (Greenwich Mean Time), or 47 equally spaced five-minute returns. Second, fixed and moving holidays, including Christmas, New Year's Day etc., and thin trading days (that is, days when the trading hours did not fully cover the time window of 14:35 GMT to 18:30 GMT) are excluded from the sample. Considering all exclusions, this leaves us with 2319 complete trading days for the construction of the final set of covariance matrices. As our measure of realised covariance, we use an estimate of the integrated covariance. The integrated covariance is the contribution to the quadratic variation process that is due to the continuous part of the underlying continuous time process. For estimation we therefore disentangle the continuous from the jump component. The details are outlined in [Appendix A](#). Since the realised covariance estimator does not necessarily lead to positive-definite covariance matrices, we check for the positive-definiteness of the covariance matrices. If there is a violation, we replace the estimate by the nearest positive-definite covariance matrix, using the projection algorithm of [Higham \(2002\)](#). In [Figure 1](#), we display our estimates of the realised variances, covariances and correlations of the three markets under consideration.

### 4.2. Static analysis: spillover table

We estimate the model in Eq. (1) and apply the sequential elimination procedure as outlined in [Appendix B](#). For the full sample, the SER procedure based on the Schwarz criterion sets 61 of the 114 parameters to zero. In [Table 1](#), we provide the spillover table for the full sample and a forecast horizon<sup>4</sup> of  $H = 25$  days. Analogously, we also apply the SER procedure to the MHAR-RV model and provide the corresponding spillover table in [Table 2](#). The spillover

---

<sup>3</sup><http://www.tickdata.com>

<sup>4</sup>We focus on a forecast horizon of  $H = 25$  days. However, we also examine a range of different forecast horizons as robustness checks.

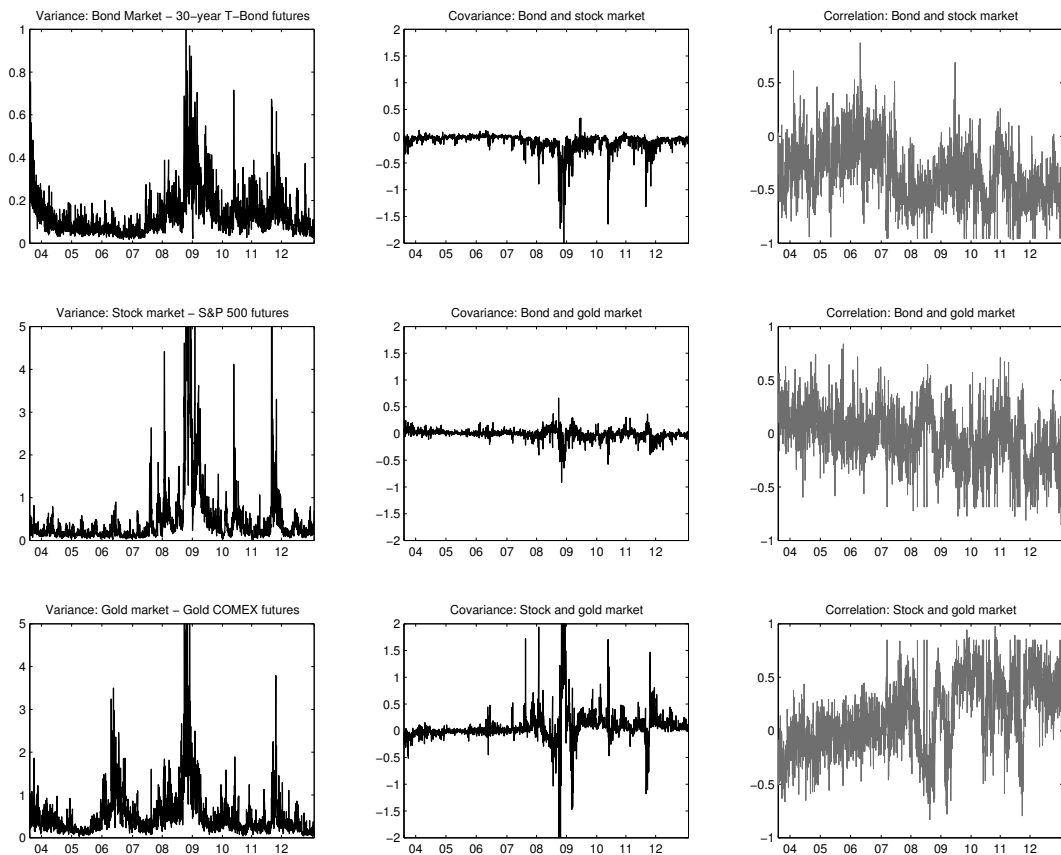


**Figure 1: Daily realised (co)variances.** Top panel: realised variance of the bond market and realised covariance and realised correlation between the bond and the stock market. Middle panel: realised variance of the stock market and realised covariance and realised correlation between the bond and the gold market. Bottom panel: realised variance of the gold market and realised covariance and realised correlation between the stock and the gold market.

table contains the variance decomposition where the forecast-error variance components in forecasting variable  $i$  coming from shocks to variable  $j$  (for all  $i$  and  $j$ ) are reported. The  $ij$ th entry in the table is the approximate contribution to the forecast-error variance of the realised (co)variance  $i$  coming from innovations to the realised (co)variance  $j$ . It also includes the spillover index in the lower right corner. The off-diagonal column sums labelled "directional TO others" and the off-diagonal row sums labelled "directional FROM others" represent the directional spillovers; see Diebold and Yilmaz (2012, 2014).

A number of features should be noted in Table 1. For the pairwise directional spillovers, we find clear blocks of high and low pairwise directional spillovers. For example, the variance of the bond market ( $Var_{US}$ ) and the covariance between the bond and the stock market ( $Cov_{US,SP}$ ) exhibit substantial pairwise directional spillovers (26% and 15%, respectively). Similarly, we find high pairwise directional spillovers of 29% and 24% for the variance of the

**Table 1:** Spillover table for the full sample

	$Var_{US}$	$Cov_{US,SP}$	$Cov_{US,GC}$	$Var_{SP}$	$Cov_{SP,GC}$	$Var_{GC}$	Directional FROM others
$Var_{US}$	0.5271	0.2634	0.0152	0.1029	0.0235	0.0678	0.4729
$Cov_{US,SP}$	0.1545	0.4870	0.0194	0.2424	0.0186	0.0781	0.5130
$Cov_{US,GC}$	0.0035	0.0299	0.6252	0.0396	0.2849	0.0170	0.3748
$Var_{SP}$	0.1065	0.2872	0.0071	0.4927	0.0018	0.1047	0.5073
$Cov_{SP,GC}$	0.0152	0.0128	0.2099	0.0607	0.6712	0.0302	0.3288
$Var_{GC}$	0.0635	0.1345	0.0076	0.1211	0.0203	0.6530	0.3470
Directional TO others	0.3432	0.7279	0.2592	0.5667	0.3491	0.2978	Spillover index <b>0.4240</b>
Net spillovers	-0.1297	0.2149	-0.1156	0.0593	0.0203	-0.0493	

**Notes:** The table shows the variance decomposition for the full sample (from July 2003 to December 2012) for a forecast horizon of  $H = 25$  days based on the MHAR-RCov model. The  $ij$ th entry in the table is the approximate contribution to the forecast-error variance of the realised (co)variance  $i$  coming from innovations to the realised (co)variance  $j$ .

**Table 2:** Spillover table for the full sample

	$Var_{US}$	$Var_{SP}$	$Var_{GC}$	Directional FROM others
$Var_{US}$	0.7907	0.1670	0.0424	0.2093
$Var_{SP}$	0.1401	0.7249	0.1350	0.2751
$Var_{GC}$	0.0436	0.1560	0.8004	0.1996
Directional TO others	0.1838	0.3230	0.1773	Spillover Index 0.2299

**Notes:** The table shows the variance decomposition for the full sample (from July 2003 to December 2012) for a forecast horizon of  $H = 25$  days based on the MHAR-RV model.

stock market ( $Var_{SP}$ ) and the covariance between the bond and the stock market ( $Cov_{US,SP}$ ). Of lower magnitude, but still substantial, are the pairwise directional spillovers between the variance of the gold market ( $Var_{GC}$ ) and the covariance between the bond and the stock market ( $Cov_{US,SP}$ ). Hence, spillovers from the covariance between the bond and the stock market ( $Cov_{US,SP}$ ) to the variances and vice versa are substantial and relevant. We also find notable pairwise directional spillovers among the variances and covariances. For example, we find pairwise directional spillovers of 10% and 11 % among the variance of the bond market ( $Var_{US}$ ) and the stock market ( $Var_{SP}$ ), and of 28% and 21% among the covariances involving the gold market ( $Cov_{US,GC}$  and  $Cov_{SP,GC}$ ). Nevertheless, the largest individual elements are the diagonal elements, that is the own variance shares. In contrast, we find rather low pairwise directional spillovers across the two covariances involving the gold market and the three variances.

The row sum of the pairwise directional spillovers in [Table 1](#) yields the directional spillovers from others. Similarly, the column sum of the pairwise directional spillovers results in the directional spillovers to others. We consider first the “directional FROM others” column. The highest directional spillovers go to the covariance between the bond and the stock market ( $Cov_{US,SP}$ ) and to the variance of the stock market ( $Var_{SP}$ ), while the covariance between the gold and the stock market ( $Cov_{SP,GC}$ ) receives the smallest directional spillovers. Moreover, the variance of the gold market, as well as the two covariances involving the gold market, receive substantially less spillovers ( $< 37\%$ ) than the other variances and covariances ( $> 47\%$ ). Considering the “directional TO others” row, we find a similar pattern. More specifically, we find that the covariance between the bond and the stock market ( $Cov_{US,SP}$ ) is the most relevant spillover transmitter. This is because the most substantial spillovers (73%) originate from the covariance between the bond and the stock market ( $Cov_{US,SP}$ ). In contrast, the variance of the gold market ( $Var_{GC}$ ) and the covariance between the bond and the gold market ( $Cov_{US,GC}$ ) are the least relevant spillover transmitters (26% and 30%). Thus, together with the covariance between the stock and the gold market ( $Cov_{SP,GC}$ ), they are not only the least relevant spillover receivers, but also the least relevant transmitters. The gold market can hence be considered as a market that is less subject to systemic risk. In contrast, the stock and bond market are substantially exposed to spillovers, which emphasises the strong linkages between these two markets.

The system-wide spillovers of the realised covariance matrix are measured by the spillover index in the lower right boldface entry of [Table 1](#). The spillover index measures the systemic risk associated with the multivariate system. A spillover index of 43% means that 43% of the covariance forecast-error variance comes from spillovers. This illustrates how highly interconnected the variances and covariances of the three markets are. In contrast, for the MHAR-RV model [Table 2](#) reports a substantially lower spillover index of 23%. Thus, the spillover index of the MHAR-RCov model is almost twice the size of the spillover index based on the MHAR-RV model. This shows that neglecting covariances underestimates the systemic risk associated with an investment in these three markets.

In order to evaluate the relevance of the covariances, we evaluate the contributions of the variances and the covariances. We therefore define *own covariance spillovers* as the spillovers from covariances to covariances and *cross covariance spillovers* as the spillovers from covariances to variances, in the spirit of [Eq. \(13\)](#) and [Eq. \(14\)](#). Analogously, we define *own variance spillovers* and *cross variance spillovers*. We report their contributions for the full sample in [Table 3](#). The contribution of the own variance and the own covariance spillovers amounts to 22% and 23%, respectively. They thus contribute equally to the spillover index. In contrast, the contribution of the cross covariance spillovers (30%) is larger than the contribution of the cross variance spillovers (25%). In terms of total contribution, the cross variance and

**Table 3:** Spillover contributions for the full sample

Cross variance spillovers	0.2520
Cross covariance spillovers	0.2991
Own variance spillovers	0.2227
Own covariance spillovers	0.2262

**Notes:** The table shows the spillover contributions to the spillover index based on the MHAR-RCov model for the full sample for a forecast horizon of  $H = 25$  days.

the cross covariance spillovers account for 55% (=25%+30%) of the spillover index. Consequently, more than half of the spillover index is attributable to spillovers between variances and covariances, emphasising not only their strong interdependence, but also explaining the substantially higher spillover index found using the MHAR-RCov model.

### 4.3. Dynamic analysis: spillover plot

The spillover table provides only a summary of the average spillovers. In order to account for time-variation, we move from a static sample analysis to a dynamic sample analysis. As Diebold and Yilmaz (2014) argue, allowing for time-varying spillovers effectively means allowing for time-varying parameters. Although there are several ways of introducing time-varying parameters, Diebold and Yilmaz (2009, 2012, 2014) use the rolling window approach because of its simplicity and its coherence with a wide variety of time-varying parameter mechanisms. We also follow this idea. We recursively estimate and apply the SER procedure to the MHAR-RCov and the MHAR-RV model using 500-day rolling windows<sup>5</sup>, and subsequently plot the corresponding time series of spillover indexes. We provide two spillover plots: the spillover plot based on the MHAR-RCov model, in Figure 2, and the spillover plot based on the MHAR-RV model, in Figure 3. Moreover, we focus on a time horizon of  $H = 25$  days, but also report the results for the time horizons of  $H = 2, 10$  days as robustness checks.

Comparing Figure 2 with Figure 3, we can make three observations. First, there is a noticeable level difference in the spillovers. On average, the spillover index based on the MHAR-RCov model is about 17 percentage points higher. In the same way as for the static analysis, the spillover plots confirm that the true systemic risk associated with an investment in the stock, the bond and the gold market is severely underestimated when covariances are neglected. Second, both spillover plots document an overall increase in spillovers, reflecting an increased interdependence during the financial and sovereign debt crises. As has been argued by Castiglionesi, Feriozzi and Lorenzoni (2009), Battiston, Gatti, Gallegati,

<sup>5</sup>Diebold and Yilmaz (2012) use 200-day rolling samples in their analysis. However, our MHAR-RCov model has 114 parameters to estimate in a first step so that 500-day rolling windows appears to be more reasonable. For the rolling window estimates, the SER procedure based on the Schwarz criterion sets 70% of the coefficients to zero, on average.



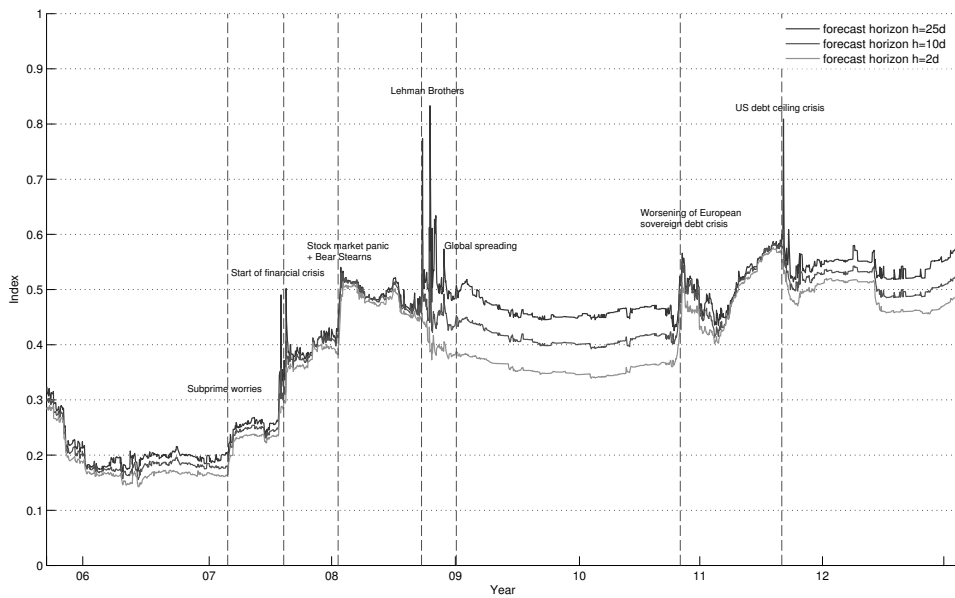


**Figure 2: Spillovers plot with covariances.** The figure depicts the spillover plot for different forecast horizons  $H = 2, 10, 25$  days. Each point corresponds to the spillover index derived from a recursively estimated and restricted MHAR-RCov model using 500-day rolling windows.

Greenwald and Stiglitz (2012), and Billio, Getmansky, Lo and Pelizzon (2012), this increased interdependence reflects the vulnerability to systemic events of tightly connected markets. In other words, the tighter the connections are, the higher the impact of systemic events such as those witnessed during the recent financial and sovereign debt crises. Third, the spillover plots based on the MHAR-RCov model and on the MHAR-RV model share similar dynamics and react to the same major economic events, with two notable exceptions. The spillover index based on the MHAR-RV model displays a delayed reaction to both the financial crisis and the US debt ceiling crisis. The spillover index based on the MHAR-RV model suddenly reacts to a particular event, such as the collapse of Lehman Brothers in September 2008 or the US downgrading in August 2011, by jumping to a new level, whereas the spillover index based on the MHAR-RCov model anticipates these new spillover levels at an earlier stage.

We now describe the time-varying behaviour of the spillover index for both models in more detail. Considering first the spillover plot with covariances in Figure 2, we find that the spillover index starts at a value of around 30%. It reacts to the first signs of subprime worries as it begins to rise in February 2007 when the subprime mortgage defaults increase. However, the most active period for the spillover index starts at the beginning of the financial crisis in July 2007; this date is marked in the spillover index with a peak of around 50%. In a similar way to Diebold and Yilmaz (2012), we can document three relevant spillover periods during the subsequent financial crisis. First, from January to March 2008, the stock market panic and the Bear Stearns turmoil result in a sudden and permanent increase in the

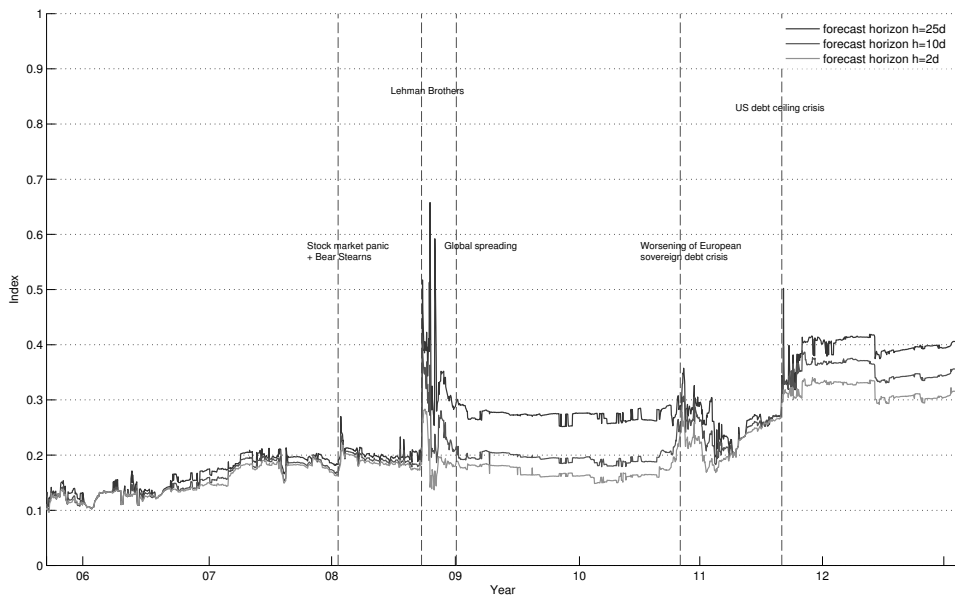


**Figure 3: Spillover plot without covariances.** The figure depicts the spillover plot for different forecast horizons  $H = 2, 10, 25$  days. Each point corresponds to the spillover index derived from a recursively estimated and restricted MHAR-RV model using 500-day rolling windows.

spillover index (of around 10 percentage points). Second, from September to December 2008, the default of Lehman Brothers causes the spillover index to peak (at over 80%). And third, after the default, the financial crisis eventually spreads around the world, as documented by the high spillover level (of around 45%). Since our sample also covers the recent sovereign debt crisis we can identify two additional relevant spillover periods. First, in the wake of the sovereign debt crisis in the second half of 2010, the spillover index based on the MHAR-RCov model marks a new spillover period when it rises above 50%. It declines temporarily to below 45% before it starts to increase noticeably in the face of the US debt ceiling crisis, which marks another period of spillovers. The spillover index peaks with the passing of the Budget Control Act and the subsequent downgrading of the United States' credit rating by Standard & Poor's at the beginning of August 2011, and after this it remains well above 50% until the end of 2012.

Turning to the spillover index based on the MHAR-RV model, as provided in **Figure 3**, we can observe that this starts at a value slightly above 10% and increases moderately until the stock market panic at the beginning of 2008. The panic in the stock market results in a sharp increase of the spillover index up to 27%, but the index quickly returns to a moderate level of 20%. After the collapse of Lehman Brothers in September 2008, the spillover index based on the MHAR-RV model displays similar dynamics to those of the spillover index based on the MHAR-RCov model, i.e., it peaks at 66% and remains high during the subsequent global spreading of the financial crisis until the second half of 2011. In contrast to the spillover plot

including covariances, the US debt ceiling crisis is reflected rather late in the spillover plot based on the model that considers only variances, as can be seen from the sudden peak of the spillover index that coincides with the downgrading of the United States' credit rating. The spillover index based on the MHAR-RV model thus reacts to the same major economic events as does the spillover index based on the MHAR-RCov model. However, it detects the financial and the US debt ceiling crises later.

In conclusion, the spillover index based on the MHAR-RCov model ranges between 17% and 83 %, while the spillover index based on the MHAR-RV model is between 10% and 66%. They both respond to major economic events during the recent financial and sovereign debt crises. Including covariances, however, leads to a higher spillover level, on average. Moreover, including covariances allows us to document the beginnings of the financial crisis and the US debt ceiling crisis at an earlier stage and more precisely than the spillover plot based on the model that includes only variances. As a consequence, modelling only variances underestimates the interdependence and the systemic risk.

#### 4.4. Dynamic analysis: own and cross spillover plots

In order to determine the relative contribution of the covariances and the variances in the dynamic setting, we provide the *cross spillover plot* in [Figure 4](#). The cross spillover plot displays the spillovers across covariances and variances in a dynamic context. The top two panels illustrate the cross variance spillovers (spillovers from variances to covariances) and the cross covariance spillovers (spillovers from covariances to variances), while the bottom panel corresponds to the difference between the cross variance and the cross covariance spillovers, i.e., the *net cross spillovers*.

Considering the cross variance and cross covariance spillovers in [Figure 4](#), we see that they share similar dynamics and are roughly of the same magnitude. The net cross spillovers confirm this observation as they are close to zero throughout our sample. Hence, both the cross variance and the cross covariance spillovers can be considered to be equally important spillover channels.

The *own spillover plot* in [Figure 5](#) is analogous to the *cross spillover plot*. The distinction between the own variance and the own covariance spillovers is of particular interest as it allows us to analyse the role of covariances better. Most importantly, the own variance spillover plot in the MHAR-RCov model setting can be considered as the analogue of the spillover plot in the MHAR-RV model setting. More precisely, like the own variance spillover plot, which displays the spillovers between variances, the spillover plot based on the MHAR-RV model contains only variances and hence only own variance spillovers. Consequently, we can evaluate the extent to which the spillover information of the MHAR-RV model is preserved in the MHAR-RCov setting, and how much information is additionally contributed by the co-

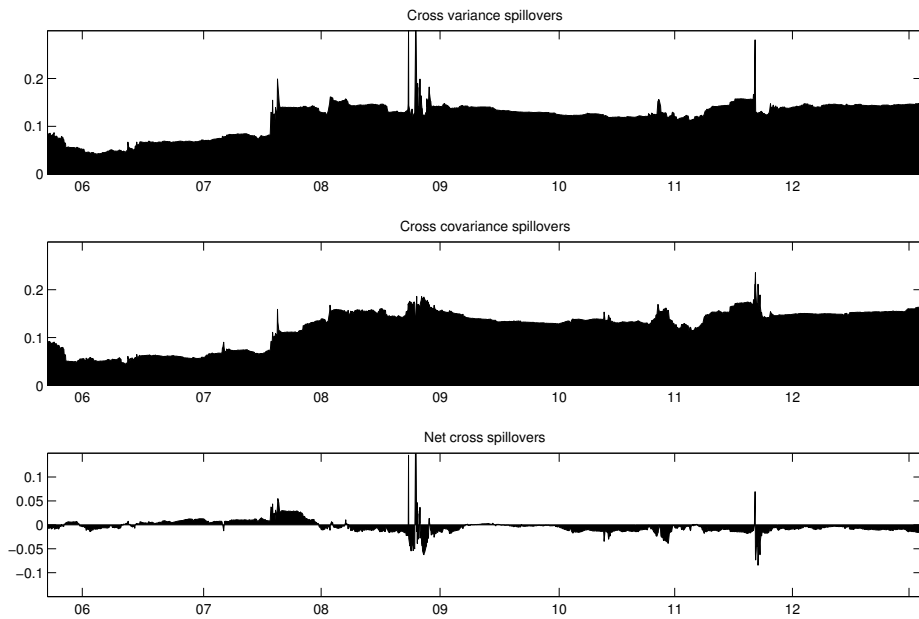


**Figure 4: Cross spillover plot.** The figure shows the cross variance, cross covariance and net cross spillovers for a forecast horizon of  $H = 25$  days based on the MHAR-RCov model. The net cross spillovers correspond to the difference between the cross variance and the cross covariance spillovers. Top panel: Cross variance spillovers. Middle panel: Cross covariance spillovers. Bottom panel: Net cross spillovers.

variances. The top two panels in [Figure 5](#) illustrate the own variance spillovers (spillovers among variances) and the own covariance spillovers (spillovers among covariances), while the bottom panel displays the *net own spillovers*.

Comparing [Figure 5](#) with [Figure 4](#), we can see that, on average, the own spillovers are of slightly smaller magnitude than the cross spillovers. Moreover, the own covariance spillover plot displays similar dynamics to the cross variance and the cross covariance spillover plots, while the own variance spillover plot reveals a different pattern. There are long periods of moderately positive net own spillovers, and shorter periods of relatively high and low negative net own spillovers ([Figure 5](#), bottom panel). More specifically, there are three episodes, during which the own variance spillovers dominate the own covariance spillovers: first, before the start of the financial crisis (2006 to mid-2007); second, during the global spreading of the financial crisis (September 2008 to the end of 2010); and third, during the US debt ceiling debate period (mid-2011 to the end of 2012). On the contrary, the periods when the own covariance spillovers exceed the own variance spillovers coincide with the emergence of the financial crisis (mid-2007 to the Lehman Brothers collapse) and of the US debt ceiling crisis (the first half of 2011). This pattern can be linked to the previous observation that only variance spillovers, as shown in the spillover plot based on the MHAR-RV model, react late to the

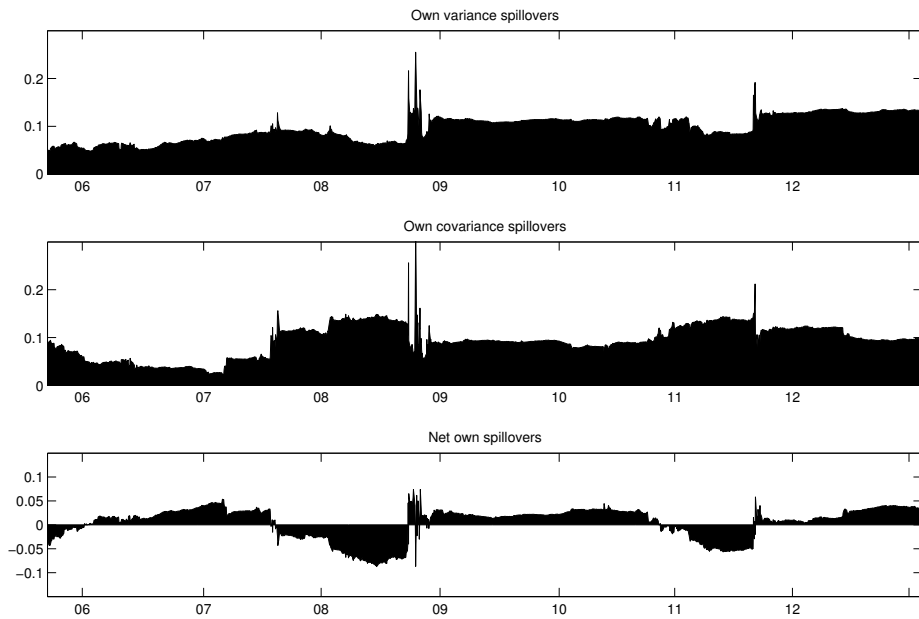


**Figure 5: Own spillover plot.** The figure shows the own variance, own covariance and net own spillovers for a forecast horizon of  $H = 25$  days based on the MHAR-RCov model. The net own spillovers corresponds to the difference between the own variance and the own covariance spillovers. Top panel: Own variance spillovers. Middle panel: Own covariance spillovers. Bottom panel: Net own spillovers.

beginnings of the financial and the US debt ceiling crises. We therefore provide in [Figure 6](#) the spillover plot based on the MHAR-RV model and the dynamics of the adjusted<sup>6</sup> own variance spillover plot. Comparing the two plots confirms that the own variance spillover plot can be considered as the analogue to the spillover plot based on the MHAR-RV model. In other words, the spillover plot based on the MHAR-RCov model contains the information provided in the MHAR-RV model.

Furthermore, by comparing [Figure 4](#) with [Figure 5](#) we can identify the following drivers of the reaction to the financial and the US debt ceiling crisis: first, the cross variance, second the cross covariance, and third the own covariance spillovers. This is because the own variance spillovers do not react to the subprime worries emerging in 2007, and remain fairly calm until the collapse of Lehman Brothers. Moreover, the own variance spillovers display a delayed reaction to the US debt ceiling crisis. Consequently, the tracking and monitoring of crises is better achieved in a setting where covariances are considered. The spillover information contained in the MHAR-RV model is clearly insufficient.

---

<sup>6</sup>Adjusted refers to decreasing the denominator to  $N = 3$  in order to make the plot comparable to the spillover plot based on the MHAR-RV model.

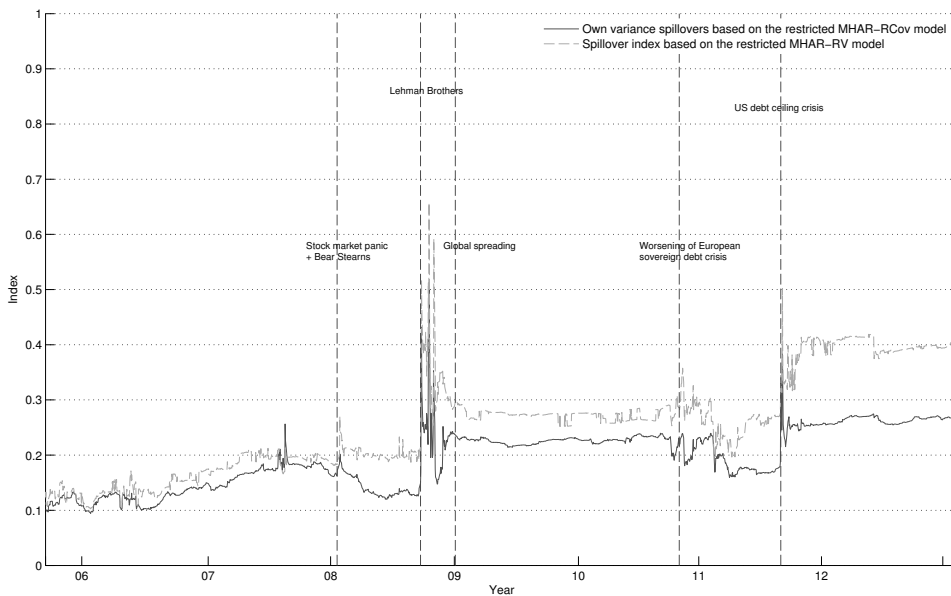


**Figure 6: Spillover comparison.** The figure depicts the adjusted own variance spillover plot (solid line) and the spillover plot based on the MHAR-RV model (dashed line) for a forecast horizon of  $H = 25$  days. Adjusted refers to decreasing the denominator to  $N = 3$  in order to make the plot comparable to the spillover plot based on the MHAR-RV model.

To sum up, the cross spillovers are of slightly larger magnitude than the own spillovers. As regards only the cross spillovers, both the cross covariance and the cross variance spillovers are equally important spillover channels, and both react early to the financial and US debt ceiling crises. Comparing the cross spillovers with the own spillovers, we find that the own covariance spillovers display a similar pattern to the cross covariance and cross variance spillovers, while the own variance spillovers differ. More specifically, the cross variance, cross covariance and own covariance spillovers are the drivers for the early reaction of the spillover index to the financial and the US debt ceiling crisis. In contrast, the spillover information from the MHAR-RV model and the own variance spillover information from the MHAR-RCov model, respectively, are not sufficient.

#### 4.5. Dynamic analysis: directional and pairwise directional spillover plots

The spillover plot, as well as the own and the cross spillover plots, give a first impression of the time-varying behaviour of the spillover index and its composition, yet they discard directional information. We therefore derive the dynamics of the directional spillovers using Eq. (13) and Eq. (14). This allows us to analyse the spillover dynamics to and from a specific source. We focus on the directional spillovers to and from variances, as we are particularly interested in how the directional spillovers to and from variances change when covariances are considered. We therefore decompose the directional spillovers into directional cross and

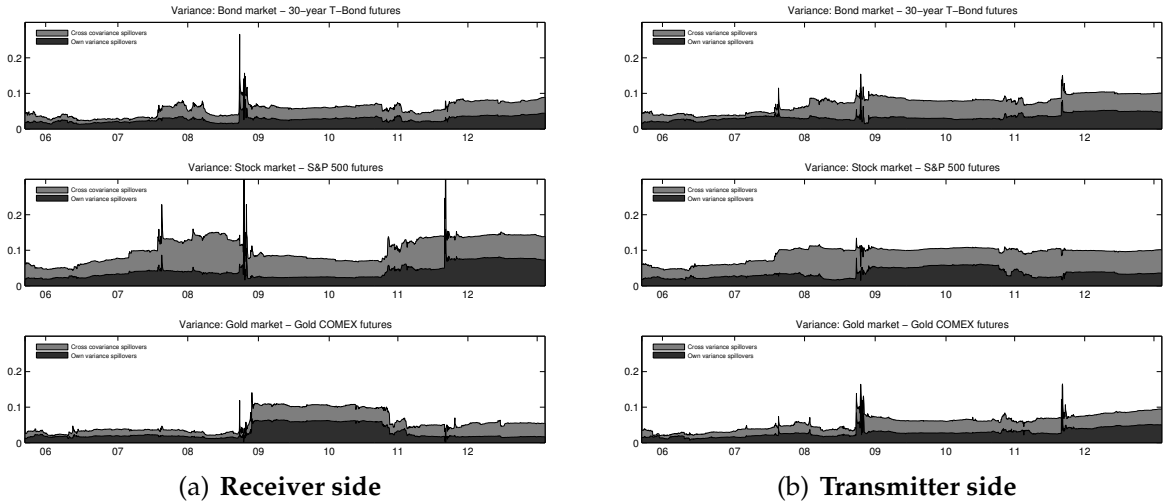


**Figure 7: Directional spillovers from and to the variances with cross and own spillover decomposition.** The figure shows the directional spillovers from and to the variances along with a directional cross and own spillover decomposition for a forecast horizon  $H = 25$  days based on the MHAR-RCov model. The left column displays the directional spillover to the variances (receiver side). It further decomposes these directional spillovers into directional own variance spillovers (dark grey area) and directional cross covariance spillovers (light grey area). The right column depicts the directional spillovers originating from the variances (transmitter side). They are also decomposed into directional own variance (dark grey area) and directional cross variance spillovers (light grey area).

directional own spillovers, and provide the results in Figure 7. The left column displays the receiver side of the directional variance spillovers (“directionals FROM” column entries), while the right column shows the transmitter side (“directionals TO” row entries).

In terms of magnitude, the most relevant directional spillover receiver and transmitter is the variance of the stock market (Figure 7, middle panels), while the other two variances are spillover receivers and transmitters of smaller size (Figure 7, top and bottom panels). Moreover, the decomposition into own and cross directional spillovers reveals the importance of the directional cross spillovers for all three variances (Figure 7, light grey areas). They are not only substantial, but they clearly dominate the directional spillovers from and to the variances (Figure 7, light grey areas vs. dark grey areas). More specifically, the directional spillovers to and from the variance of the bond market react early to the financial crisis by receiving and transmitting substantially more cross spillovers from the start of the financial crisis in mid-2007 until the end of 2012 (Figure 7, top panels, light grey areas). For the stock market, we can observe a similar pattern (Figure 7, middle panels, light grey areas vs. dark grey areas): the directional spillovers from and to the variance of the stock market are also mainly driven by cross spillovers. They increase early in 2007 and gain momentum with the

emergence of the financial crisis in mid-2007. Subsequently, they temporarily decline during the global spreading of the financial crisis, and increase again with the emerging US debt ceiling crisis at the beginning of 2011 (Figure 7, middle panels, light grey areas). In contrast, the directional spillovers from and to the variance of the gold market exhibit directional own and cross spillovers that share similar dynamics until the emergence of the US debt ceiling crisis (Figure 7, bottom panels, light grey areas vs. dark grey areas). Both the directional cross and the directional own spillovers remain calm until the collapse of Lehman Brothers and they increase with the global spreading of the financial crisis. With the emerging US debt ceiling crisis, however, the directional cross spillovers to the variance of the gold market dominate the directional own variance spillovers (Figure 7, right column, bottom panel, light grey area vs. dark grey area), while the directional cross spillovers from the variance of the gold market continue to display a similar pattern to the directional own variance spillovers (Figure 7, left column, bottom panel, light grey area vs. dark grey area). In other words, the cross variance and the cross covariance spillovers, not the own variance spillovers, are the principal drivers of the early reaction.

We further decompose the directional spillovers from and to the variances into pairwise directional spillovers, using Eq. (15) and Eq. (16). This is to determine the main drivers of the dynamics in the directional spillovers to and from variances. Figure 8 provides the pairwise directional cross (variance and covariance) spillover plots, while Figure 9 reports the pairwise directional own variance spillover plots.

We start with the decomposition of the directional cross spillover plots in Figure 8. On the receiver side (Figure 8, left column), two important observations can be made. First, the main cross covariance spillover source is the covariance between the bond and the stock market (Figure 8, sum of the dark grey areas in the left column). Second, the variance of the stock market is the largest cross spillover receiver (Figure 8, left column, middle panel), and is closely followed by the variance of the bond market (Figure 8, left column, top panel). Consequently, there is a strong linkage between the covariance of the bond and the stock market and the corresponding variances. In contrast, the remaining two covariances, i.e.,  $Cov_{US,GC}$  and  $Cov_{SP,GC}$ , are a relatively negligible source of cross covariance spillovers (Figure 8, sum of the light and medium grey areas in the left column). They are mostly relevant to the variance of the stock and the gold market. We observe similar patterns on the transmitter side.

Furthermore, the pairwise directional cross spillover plots also allow us to identify different drivers of the financial and the US debt ceiling crises in the cross variance and the cross covariance spillover plots and subsequently in the spillover plot. On the receiver side, the cross covariance spillovers to the variance of the bond and the stock market (Figure 8, left column, top and middle panel) react early to the financial crisis in mid-2007 until the



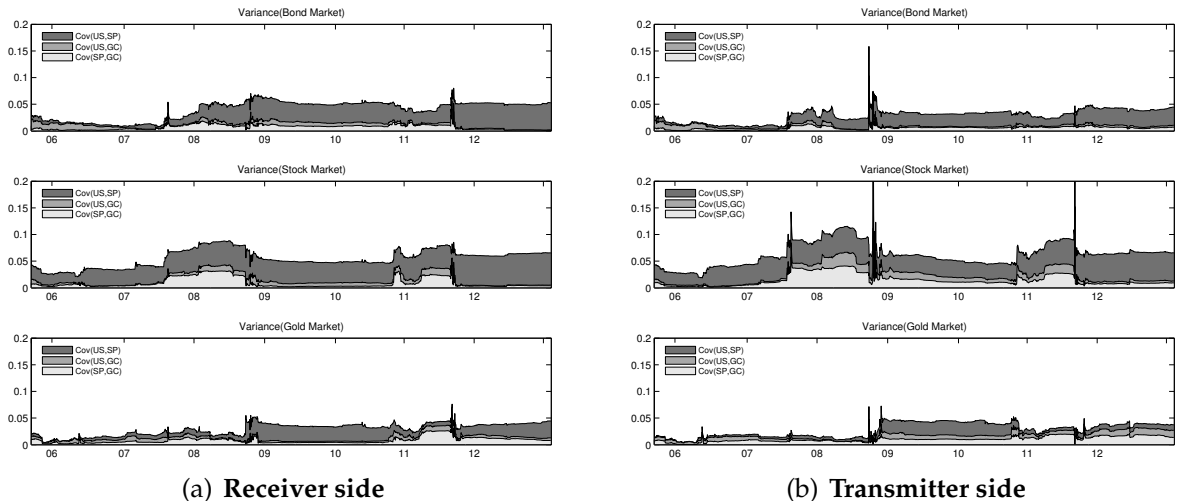


**Figure 8: Pairwise directional cross spillover plots.** The figure shows the directional cross spillovers for a forecast horizon  $H = 25$  days based on the MHAR-RCov model. The left column displays the directional spillovers to each of the variances from all the covariances (receiver side). The right column shows the directional spillovers to all covariances originating from each of the variances (transmitter side).

second half of 2008, while it is the cross covariance spillovers to the variance of the stock and the gold market (Figure 8, left column, middle and bottom panel) that lead to an early reaction to the emerging US debt ceiling crisis in the first half of 2011. In other words, the early reaction to the financial crisis is driven by spillovers coming from both the covariance between the stock and the gold market ( $Cov_{SP,GC}$ ) and the covariance between the bond and the stock market ( $Cov_{US,SP}$ ), while the early reaction to the emerging US debt ceiling crisis is entirely driven by the covariance between the stock and the gold market ( $Cov_{SP,GC}$ ). We find a similar pattern on the transmitter side of the pairwise directional cross spillovers (Figure 8, right column).

This spillover pattern might be linked to a flight-to-quality phenomenon. A flight-to-quality phenomenon occurs during financial turmoil when investors sell risky assets and buy safer assets, resulting in decreasing and negative correlations; see Chordia, Sarkar and Subrahmanyam (2005), Conolly, Stivers and Sun (2005), Baur and Lucey (2009), and Creti, Jots and Mignon (2013), among others. Although our analysis does not allow us to determine the direction in which the covariances will change, the higher spillovers indicate that the covariances either increase or decrease. Considering the relevant realised covariances in Figure 1 (middle column, top and bottom panel), we can observe that the increased cross spillover activity coincides with the episodes of substantially negative realised covariances. Simultaneously, we can also observe that the corresponding realised correlations in Figure 1 (last

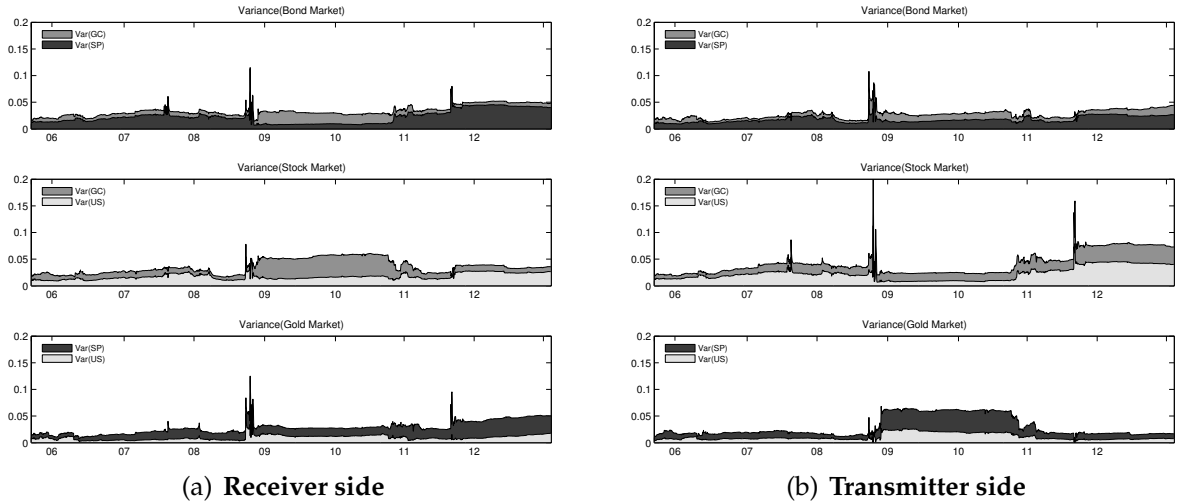


**Figure 9: Pairwise directional own variance spillover plots.** The figure shows the directional own variance spillovers for a forecast horizon  $H = 25$  days based on the MHAR-RCov model. The left column displays the directional spillovers from all the variances to each of the variances (receiver side). The right column shows the directional spillovers to all variances originating from each of the variances (transmitter side).

column, top and bottom panel) display pronounced negative trends during these episodes. Consequently, the observed spillover patterns are consistent with a flight-to-quality phenomenon. More specifically, during the first half of 2007 and in particular during the stock market panic at the beginning of 2008, the increased spillovers from and to the covariance between the bond and the stock market on the one hand and between the stock and the gold market on the other hand indicate that all three variances and the covariances involving the stock market change. This spillover pattern could be induced by investors swapping out of US equities and into US treasuries and gold. On the contrary, the emergence of the US debt ceiling crisis is mainly characterised by spillovers across the covariance between the stock and the gold market and the variance of the stock and the gold market. This observation could be associated with investors fleeing into the gold market, since the bond market might have been perceived as a less safe investment in the wake of the US debt ceiling crisis.

We also analyse the directional own variance spillovers provided in Figure 9. In contrast to the previous directional (variance and covariance) cross spillover plots in Figure 8, the dynamics of the directional own variance spillovers on the receiver and the transmitter side do not exhibit a similar time evolution for all markets. For the variance of the stock and the gold market, we observe an asymmetric pattern (Figure 9, middle and bottom panels). Consider first the variance of the stock market. On the receiver side, the variance of the stock market starts to receive substantially more own variance spillovers with the Lehman

Brothers collapse (Figure 9, left column, middle panel). In contrast, on the transmitter side, the directional own variance spillovers decline with the Lehman Brothers collapse (Figure 9, right column, middle panel). Moreover, for the US debt ceiling crisis, we observe that the directional own variance spillovers substantially increase on the transmitter side, while they decline on the receiver side. We find the exactly opposite directional own spillover pattern on the receiver and on the transmitter side of the gold market's variance (Figure 9, bottom panels). Consequently, the variance of the gold market receives substantially more own variance spillovers in mid-2011 (Figure 9, left column bottom panel), while it is the variance of the stock market that transmits more directional own variance spillovers with the downgrading of the US credit rating in mid-2011 (Figure 9, right column, middle panel). Finally, and in contrast to variance of the stock and the gold market, the directional own variance spillovers to and from the variance of the bond market (Figure 8, top panels) display similar directional own variance spillover dynamics on the receiver and the transmitter side.

The decomposition into pairwise directional own variance spillovers reveals that these own variance spillover patterns are intertwined. The reaction to the financial crisis of the directional own variance spillovers on the receiver side is due to the increased directional own variance spillovers to the stock market's variance (Figure 9, left column, middle panel, period from mid-2009 until end of 2011). These substantially higher directional own variance spillovers originate from the variance of the gold market (Figure 9, right column, bottom panel, dark grey area, period from mid-2009 until end of 2011). In contrast, the reaction to the US debt ceiling crisis on the receiver side is due to higher directional spillovers to the variance of the bond and the gold market (Figure 9, left column, top and bottom panel, period from mid-2011 until end of 2012) originating from the variance of the stock market (Figure 9, right column, medium panel, light and medium grey area, period from mid-2011 until end of 2012). In other words, during the financial crisis, the variance of the gold market transmits more spillovers than it receives, and the variance of the stock market receives more of these spillovers than it transmits. The reverse pattern can be observed for the US debt ceiling crisis. The variance of the stock market transmits more spillovers to the variance of the gold and the bond markets than it receives from them (Figure 9, left column, top and bottom panels, dark grey areas vs. left column, middle panel, medium and light grey area, period from mid-2011 until end of 2012). Together with the cross spillover analysis, we can therefore conclude that the late reaction to the financial and US debt ceiling crisis in the own variance spillover plots in Figure 5 is mainly due to the delayed own variance spillovers between the variance of the stock and the gold market.

Furthermore, we analyse in more detail whether the spillover information from the MHAR-RV model is contained in the MHAR-RCov model. We therefore provide the (pairwise) directional own variance spillover plots based on the MHAR-RV model in Figure 10. Com-

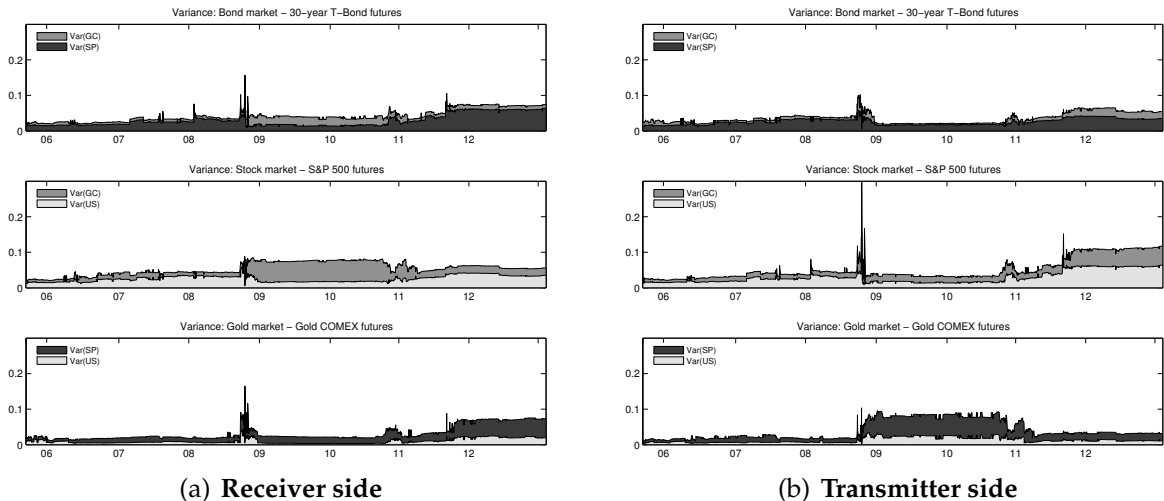


**Figure 10: Adjusted pairwise directional own variance spillovers.** The figure depicts the adjusted directional own variance spillovers for a forecast horizon of  $H = 25$  days based on the MHAR-RV model. Adjusted refers to increasing the denominator to  $N = 6$  in order to make the plot comparable to the directional spillover plots based on the MHAR-RCov model. The left column displays the directional spillovers from all variances to each of the variances (receiver side). The right column shows the directional spillovers to all variances originating from each of the variances (transmitter side).

paring the (pairwise) directional own variance spillover plots based on the MHAR-RCov model in Figure 9 with the (pairwise) directional own variance spillover plots based on the MHAR-RV model in Figure 10, we find strong similarities. This implies that the spillover information inherent to variances is preserved in the directional spillover analysis based on the MHAR-RCov model. Moreover, our (pairwise) directional spillover analysis has shown that the spillovers across variances and covariances are meaningful, and that they allow us to track the events witnessed during the recent financial and sovereign debt crises better. Consequently, in excluding covariances, one misses an important spillover channel essential to all three variances.

## 5. Conclusion

This paper investigates the role of covariances in the transmission mechanism of variance spillovers, using the spillover measures introduced by Diebold and Yilmaz (2012, 2014). In order to do this, we provide a comparative analysis for a model including covariances and a model excluding covariances. We perform the spillover analysis on three asset classes (equity, fixed income and gold) over a period of almost ten years.

The spillover analysis shows the significance of the covariances. First, the spillover measure based on the model including covariances displays a higher overall level compared with the spillover measure based on the model that considers only variances. To ignore covariances is thus to underestimate the systemic risk associated with an investment in the three asset classes. Moreover, the time evolution of the spillover measure including covariances detects the beginnings of the financial and the US debt ceiling crises earlier than the spillover measure that only considers variances. We find that the cross variance, cross covariance and own covariance spillovers are the main drivers for these early reactions. In other words, the spillover information from the variances only is not sufficient. Ignoring covariances thus results in a major loss of spillover information that is relevant to all three variances.

The decomposition of the directional spillovers to and from variances into (pairwise) directional own variance and (pairwise) directional cross (variance and covariance) spillovers emphasises the importance of cross (variance and covariance) spillovers. Moreover, the decomposition reveals the drivers of the early reaction to the financial and the US debt ceiling crisis in the cross variance and the cross covariance spillovers and thus also in the system-wide spillovers. The driver of the financial crisis is the covariance between the stock and the gold market as well as the covariance between the bond and the stock market, while the driver is only the first of these in the case of the US debt ceiling crisis. This particular spillover pattern might be linked to a flight-to-quality phenomenon. The cross spillovers we observe with the emergence of the financial crisis could be generated by investors fleeing out of equity into US treasuries and gold, whereas the cross spillovers observed during the emergence of the US debt ceiling crisis could be explained by investors fleeing into the gold market and to a lesser extent into the bond market.

The insights of this study are important for risk managers, asset managers and policy makers for two reasons. First, measuring spillovers across covariances and variances provides deeper insights into the spillover transmission mechanisms that are relevant to portfolio diversification. Second, evaluating variance and covariance spillovers among the stock, the bond and the gold market as opposed to only (own) variance spillovers improves the detection and tracking of crises. This allows one to adjust the risk exposures of portfolios accordingly and in good time, and may reduce the transaction costs arising from unnecessary adjustments in portfolios.

Although we perform our analysis on a small portfolio that considers only three markets, we find a substantial loss of information when we ignore covariances. We expect these losses to increase as the dimensions of the underlying universe of assets become higher. Clearly, this would require an extension of our modelling approach to larger portfolios. We leave this for future research.

## References

- Acharya, V. V., L. H. Pedersen, T. Philippon and M.P. Richardson (2010): "Measuring systemic risk," Unpublished working paper. New York University.
- Adrian, T. and M. K. Brunnermeier (2011): "CoVaR," Princeton University.
- Akaike, H. (1973): "Information theory and an extension of the maximum likelihood principle," in *2nd International Symposium on Information Theory*, edited by B. N. Petrov and F. Csáki, 267–281.
- Andersen, T. G., T. Bollerslev, F. X. Diebold and P. Labys (2003): "Modelling and forecasting realized volatility," *Econometrica*, **71**(7), 579–625.
- Battiston, S., D. D. Gatti, M. Gallegati, B. Greenwald and J. E. Stiglitz (2012): "Liaisons dangereuses: Increasing connectivity, risk sharing and systemic risk," *Journal of Economic Dynamics and Control*, **36**, 1121–1141.
- Bauer, G. H. and K. Vorkink (2011): "Forecasting multivariate realized stock market volatility," *Journal of Econometrics*, **160**, 93–101.
- Baur, D. G. and B. M. Lucey (2009): "Flights and contagion - An empirical analysis of stock-bond correlations," *Journal of Financial Stability*, **5**, 339–352.
- Billio, M., M. Getmansky, A. W. Lo and L. Pelizzon (2012): "Econometric measures of connectedness and systemic risk in the finance and insurance sectors," *Journal of Financial Economics*, **104**, 535–559.
- Bollerslev, T., R. F. Engle and J. M. Wooldridge (1988): "A capital asset pricing model with time-varying covariances," *The Journal of Political Economy*, **96**(1), 116–131.
- Bonato, M., M. Caporin and R. Angelo (2009): "Forecasting realized (co)variances with a block structure Wishart autoregressive model," Swiss National Bank.
- Brüggemann, R., H.-M. Krolzig and H. Lütkepohl (2002): "Comparison of model reduction methods for VAR processes," Discussion Papers, Interdisciplinary Research Project 373: Quantification and Simulation of Economic Processes.
- Brüggemann, R. and H. Lütkepohl (2001): *Lag selection in subset VAR models with an application to a U.S. monetary system*, Econometric Studies: A Festschrift in Honour of Joachim Frohn, LIT Verlag, Münster.
- Castiglionesi, F., F. Feriozzi and G. Lorenzoni (2009): "Financial integration, liquidity and depth of systemic crisis," Euro Area Business Cycle Network.
- Chiriac, R. and V. Voev (2011): "Modelling and forecasting multivariate realized volatility," *Journal of Applied Econometrics*, **26**, 922–947.

- Chordia, T., A. Sarkar and A. Subrahmanyam (2005): "An empirical analysis of stock and bond market liquidity," *The Review of Financial Studies*, **18**(1), 85–129.
- Conolly, R., C. Stivers and L. Sun (2005): "Stock market uncertainty and the stock-bond return relation," *Journal of Financial and Quantitative Analysis*, **40**(1), 161–194.
- Corsi, F. (2009): "A simple approximate long-memory model of realized volatility," *Journal of Financial Econometrics*, **7**(2), 174–196.
- Corsi, F., F. Audrino and R. Renò (2012): "HAR Modeling for realized volatility forecasting," in *Handbook of Volatility Models and their Applications*, edited by L. Bauwens, C. Hafner and S. Laurent, New York: John Wiley & Sons, chap. 15, 363–382.
- Creti, A., M. Jots and V. Mignon (2013): "On the links between stock and commodity markets' volatility," *Energy Economics*, **37**, 16–28.
- Diebold, F. X. and K. Yilmaz (2009): "Measuring financial asset return and volatility spillovers, with application to global equity markets," *The Economic Journal*, **119**, 158–171.
- (2012): "Better to give than to receive: Predictive directional measurement of volatility spillovers," *International Journal of Forecasting*, **28**, 57–66.
- (2014): "On the network topology of variance decompositions: measuring the connectedness of financial firms," *Journal of Financial Econometrics*, **forthcoming**.
- Engle, R. F. (2002): "Dynamic conditional correlation: a simple class of multivariate GARCH models," *Journal of Business and Economic Statistics*, **20**, 339–350.
- Engle, R. F. and B. T. Kelly (2012): "Dynamic equicorrelation," *Journal of Business & Economic Statistics*, **30**(2), 212–228.
- Engle, R. F. and K. F. Kroner (1995): "Multivariate simultaneous generalized ARCH," *Econometric Theory*, **11**(1), 122–150.
- Gilder, D., M. B. Shackleton and S. J. Taylor (2013): "Cojumps in stock prices: empirical evidence," *Journal of Banking and Finance*.
- Hannan, E. J. and B. G. Quinn (1979): "The determination of the order of an autoregression," *Journal of the Royal Statistical Society*, **B41**, 190–195.
- Higham, N. J. (2002): "Computing the nearest correlation matrix - a problem from finance," *IMA Journal of Numerical Analysis*, **22**, 329–343.
- Huang, X., H. Zhou and H. Zhu (2011): "Systemic risk contributions," Unpublished working paper 2011-08. Board of Governors of the Federal Reserve System.
- Jacod, J. and A. N. Shiryaev (1987): *Limit Theorems for Stochastic Processes*, Springer.

- Koop, G., M. H. Pesaran and S. M. Potter (1996): "Impulse response analysis in nonlinear multivariate models," *Journal of Econometrics*, **74**(1), 119–147.
- Kumar, M. (2013): "Returns and volatility spillover between stock prices and exchange rates: Empirical evidence from IBSA countries," *International Journal of Emerging Markets*, **8**(2), 108 – 128.
- Lee, S. S. and P. A. Mykland (2008): "Jumps in financial markets: A new nonparametric test and jump dynamics," *Review of Financial Studies*, **21**(6), 2535–2563.
- Louzis, D. P. (2013): "Measuring return and volatility spillovers in Euro area financial markets," Bank of Greece.
- Lütkepohl, H. (2005): *New Introduction to Multiple Time Series Analysis*, Springer-Verlag.
- Pesaran, M. H. and Y. Shin (1998): "Generalized impulse response analysis in linear multivariate models," *Economics Letters*, **58**(1), 17–29.
- Schwarz, G. (1978): "Estimating the Dimension of a Model," *Annals of Statistics*, **6**, 461–464.



## A. realised (co)variance and (co)jump detection

Suppose that a  $d$ -dimensional log-price process  $X = (X^{(1)}, \dots, X^{(d)})$  follows:

$$X(t) = \int_t^t a(u)du + \int_0^t \sigma(u)dW(u) + \sum_{i=1}^{N(t)} J_i, \quad (17)$$

where  $a$  is a vector of predictable and locally bounded drifts,  $\sigma$  is a càdlàg volatility matrix process bounded away from zero,  $W$  is a vector of Brownian motions,  $N$  is a counting process, and  $J_i$  is a vector of jumps with the properties that  $N(t) < \infty$  for all  $t < \infty$  and  $\sum_{i=1}^{N(t)} J_{i,j}^2 < \infty$  for all  $j = 1, \dots, d$ .

The quadratic covariation process of the log-price process<sup>7</sup> is defined as:

$$QC_t = \int_0^t \Sigma(u)du + \sum_{i=1}^{N(t)} J_i J_i^\top, \quad (18)$$

where  $\Sigma = \sigma\sigma^\top$  and the integrated covariance is given by the first term, i.e.,

$$ICov_t = \int_0^t \Sigma(u)du. \quad (19)$$

An estimate of (18), which is a measure of the ex-post variation of the process of interest, is called the realised covariance (RC). By definition, the simplest consistent estimator of RC is the sum of the outer products of the vectors of discretely observed log returns. This is the so-called classical or naive estimator, and its properties are summarised in Andersen, Bollerslev, Diebold and Labys (2003).

In order to estimate the integrated covariance consistently, we disentangle jumps from the continuous part, based on the jump detection test outlined in Lee and Mykland (2008). Taking one day as the unit of time measurement, we estimate the daily integrated covariance by:

$$\widehat{ICov}_t = \widehat{QC}_t - \widehat{JCov}_t, \quad (20)$$

---

<sup>7</sup>The quadratic covariation process of  $X_t$  is defined as

$$[X_t] = p - \lim_{n \rightarrow \infty} \sum_{k=1}^M \{X(t_k) - X(t_{k-1})\} \{X(t_k) - X(t_{k-1})\}^\top,$$

with  $M$  denoting the equally spaced time points during the time period under consideration and  $0 = t_0 \leq t_1 < \dots < t_M = t$  being a partition such that  $\sup_k \{t_{k+1} - t_k\} \rightarrow 0$  as  $M \rightarrow \infty$ ; see Jacod and Shiryaev (1987).

where

$$\widehat{ICov}_t = \sum_{k,l=1}^P \sum_{i=1}^M (r_{i,t,k} r_{i,t,l}^\top) \mathbb{1}_{(\text{Cojump}_{i,t,k,l} > 0)} - \frac{M_t^{CJ}}{M - M_t^{CJ}} ICov_t^c, \quad (21)$$

$$\widehat{ICov}_t^c = \sum_{k,l=1}^P (r_{i,t,k} r_{i,t,l}^\top) \mathbb{1}_{(\text{Cojump}_{i,t,k,l} = 0)}, \quad (22)$$

where  $r_{i,k,t}$  for  $k, = 1, \dots, P$  denotes the intraday return of the asset  $k$  for interval  $i$  of day  $t$ ,  $\mathbb{1}_{(\cdot)}$  is an indicator function taking the value one when a cojump in assets  $k$  and  $l$  in interval  $i$  is detected<sup>8</sup> and  $M^{CJ}$  denotes the number of cojumps in day  $t$ . The correction term is designed to correct the total quadratic covariation due to cojumps by an average level of integrated covariance measured on the non-cojump returns. For cojump detection we use the following exceedance rule, as in [Gilder, Shackleton and Taylor \(2013\)](#):

$$\sum_{i=1}^M \mathbb{1}_{(\text{cojump}_{i,t,k,l})} \begin{cases} > 0 & \begin{cases} k \neq l & \text{cojump} \\ k = l & \text{jump} \end{cases} \\ = 0 & \text{no cojump or jump.} \end{cases} \quad (23)$$

## B. Model selection

Since the multivariate model in (4) suffers from the curse of dimensionality, we need to reduce the parameter space. We therefore impose restrictions on the general model by following a so-called subset procedure, in order to arrive at a more parsimonious model; see [Brüggemann and Lütkepohl \(2001\)](#) and [Brüggemann \*et al.\* \(2002\)](#). Subset modelling procedures are restriction strategies that impose restrictions on a general model along a specific path determined by a sequence of  $t$ -tests or a model selection criterion such as the information criterion introduced by [Akaike \(1973\)](#) AIC, by [Hannan and Quinn \(1979\)](#) HQ or by [Schwarz \(1978\)](#) BIC. The subset modelling procedures impose zero restrictions on the coefficients of a VAR( $p$ ) sequentially and on the basis of the best performing restriction in each step. We focus on the single equation approaches where several selection procedures are available, namely the sequential elimination of regressors (SER), the full search, the top-down and the bottom-up strategies. Among these, the SER procedure is the most compelling from the perspective of computational feasibility and order independence. The SER procedure sets coefficients to zero based on the  $t$ -ratios. The procedure sequentially eliminates the regressors with the smallest absolute  $t$ -ratios. One estimates each equation in the VAR model separately, and eliminates<sup>9</sup> the regressor with the smallest absolute value until all  $t$ -ratios are greater than some threshold  $\eta$ . Note that only one regressor at a time is eliminated. More formally, let  $L$  be the number of regressors in the model and  $t_i^{(j)}$  be the  $t$ -value associated

<sup>8</sup>If  $k = l$ , a cojump corresponds to a jump as stated in the exceedance rule (23).

<sup>9</sup>Eliminates refers to setting a coefficient to zero. Therefore, restricted least squares as outlined in [Lütkepohl \(2005\)](#) is applied in order to estimate each equation recursively.

with a specific coefficient  $\phi_l$  in the  $j$ -step, SER then deletes a regressor if and only if:

$$|t_l^{(j)}| = \min_{i=1, \dots, L-j+1} |t_i^{(j)}| \quad \wedge \quad |t_l^{(j)}| \leq \eta \quad (24)$$

and stops if all  $|t_l^{(j)}| > \eta$ . Brüggemann and Lütkepohl (2001) have shown that this strategy is equivalent to the sequential elimination based on a model selection criterion for a suitably chosen threshold  $\eta$ . Setting  $\eta = \{\exp(c_T/T) - 1\}(T - L + j - 1)^{1/2}$  in the  $j$ -th step of the elimination procedure based on  $t$ -ratios leads to the same final model as if one had sequentially reduced a given model using a model selection criterion. The threshold value  $\eta$  depends on the selection criterion via  $c_T$ , the sample size  $T$  and the number of regressors  $L$  in the model. For the different criteria, the  $c_T$  sequences are:  $c_T(AIC) = 2$ ,  $c_T(HQ) = 2 \ln \ln T$  and  $c_T(BIC) = \ln T$ . The BIC criterion selects models with more zero restrictions than the HQ and AIC, while HQ induces more restrictions than AIC. We performed the SER procedure with all three criteria. The subsequent spillover analysis does not change substantially if another criterion is used. However, the BIC criterion allows us to obtain a clearer picture of the relevant regressors. We therefore use the SER procedure with the BIC criterion.